UCRL-90742
PREPRINT
CONF-840977--1

Granular Flow Along the Interior Surface of Rotating Cones

John H. Pitts
Otis R. Walton

This paper was prepared for submittal to
8th International CHISA Meeting
Prague, Czechoslovakia
September 3-7, 1984

April 26, 1984

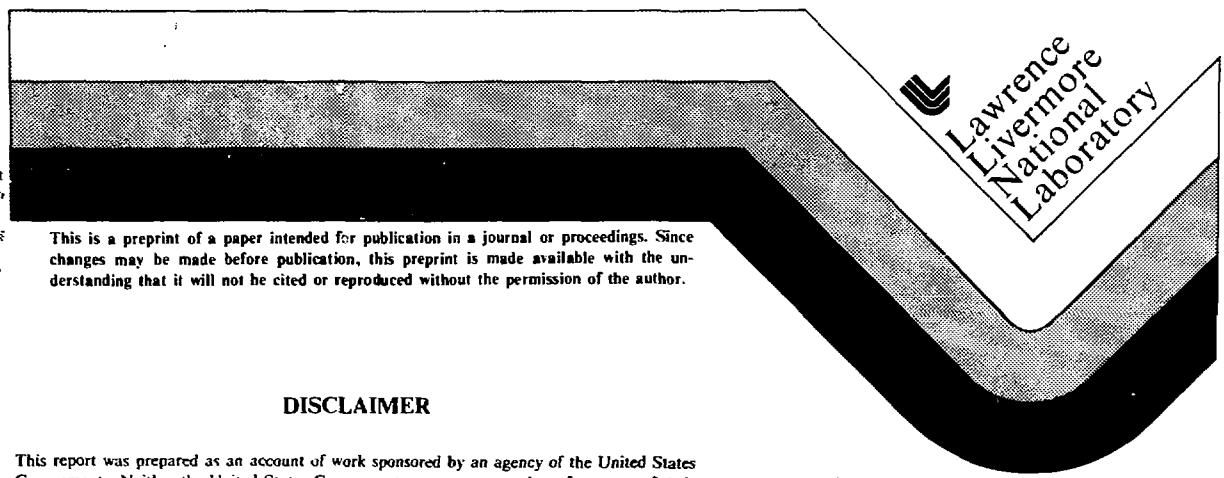

DISCLAIMER

Granular flow along the interior surface of rotating cones

John H. Pitts and Otis R. Walton
Lawrence Livermore National Laboratory, P.O. Box 5508, Livermore, California 94550, USA

Summary

Relationships are developed between the effective cone half-angle, α_{eff}, and the actual cone half-angle, α, for subcritical flow of granular material along the inside surface of a rotating cone. Rotational speed must be high enough to keep the granular material against the wall. If α_{eff} is between the wall friction angle, ϕ_w and the angle of repose, ϕ_r, the flowrate may be controlled at the exit and depends on the exit aperture area and the rotational speed.

Laboratory experiments show that exit control is possible over the entire range of effective cone half-angles from $\phi_w < \alpha_{eff} < \phi_r$ and even beyond these limits. The most uniform thickness of granular material is obtained when the cone half-angle is close to ϕ_r.

Introduction

Granular flow on the interior surface of rotating cylinders has long been used in industrial processes. Large cylindrical kilns used for manufacturing cement rotate slowly with one end elevated slightly above the other. Granular material is heated and processed into cement as it tumbles from one end to the other of the rotating cylinder. Horizontally oriented ore crushers, as large as 8 m in diameter, produce a grinding action between steel balls and ore inside the crusher as it rotates.

Our interest in granular flow in rotating chambers is for a different application--a reaction chamber concept for converting inertial-confinement-fusion energy into electrical power. In this concept, which we call Cascade[1,2,3] (see Fig. 1), a 5-m-radius double-cone-shaped chamber rotates on its horizontal axis. The chamber contains a 1-m-thick cascading blanket made of solid-lithium-ceramic granules that breeds tritium, acts as a heat transfer medium, and protects the chamber wall from fusion neutrons, x rays, and fusion-fuel pellet debris. Sand-grain-sized granules are

*Work performed under the auspices of the U. S. Department of Energy by the Lawrence Livermore National Laboratory under contract number W-7405-ENG-48.

injected into the small ends of the chamber at a temperature of 800 K and are held against the wall in a loosely-packed blanket by the centrifugal action of the rotating chamber. As the granules cascade along the wall, they absorb heat from the fusion reactions, and flow out through apertures into a stationary granule catcher at a temperature of 1200 K. They are then directed to heat exchangers for energy extraction after which they are reinjected into the chamber. The open ends of the chamber act as vacuum and beam ports. They also provide space for the injection of 600-MJ fusion-fuel pellets at 5 Hz, illuminated by laser or ion beams as each one reaches the chamber center.

During our development of Cascade, we raised several questions concerning the chamber shape, the feasibility of maintaining a uniform 1-m-thick granule blanket, and the mixing of the granules within the blanket. We analyzed the granular flow behavior[4] and conducted a series of simple small-scale laboratory experiments to answer some of these questions. This paper discusses our analytical and experimental efforts.

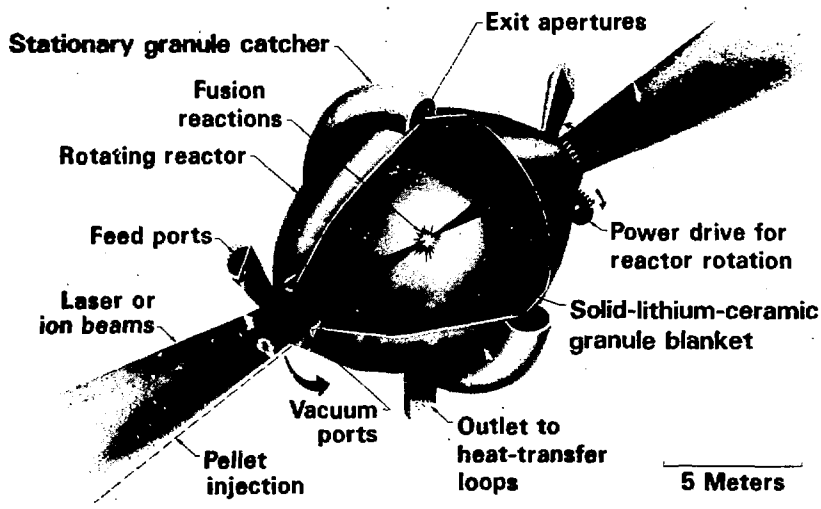

Fig. 1 Cascade: a centrifugal-action, solid-lithium-ceramic granule blanket reactor.

Granular Flow Phenomena

Two different types of granular flow are possible: supercritical flow, in which the velocity of the flowing material is higher than the wave propagation velocity through the bulk material, and subcritical (or quasi-static) flow, in which a disturbance can be propagated upstream. We restricted our analysis to subcritical flow because our maximum velocity in the Cascade chamber is on the order of 100 mm/s--far less than wave propagation velocities in loose porous granular materials, which are typically on the order of meters per second.

Subcritical flow on an incline exhibits behavior in which the flowrate can be totally controlled from a downstream position, making it possible to stop the flow while the material remains on an incline. Further, the thickness of the material on the incline can be controlled independently by the height of the inlet opening through which the material flows. This type of flow is particularly well suited for the Cascade chamber because continuous movement of thick layers, with easy control of the flow parameters, is feasible.

Subcritical flow of cohesionless granular materials can be obtained by restricting the outlet if the following condition is satisfied:

$$\phi_w < \alpha_i < \phi_r. \qquad (1)$$

where α_i = angle of incline

ϕ_w = wall friction angle (above which sliding will occur)

ϕ_r = angle of repose for the material.

For ceramic materials on a machined metal surface, the likely ranges of the wall friction angle and the angle of repose are $20° < \phi_w < 32°$ and $24° < \phi_r < 40°$. With a conical chamber where the rotational speed is high enough to hold the granules against the wall, we must use an effective angle of incline, α_{eff}, in Equation (1), which depends on the total body force acting on the material, including gravity, centrifugal and Coriolis forces as well as on the shape and orientation of the chamber itself.

Material will slide on the inner surface if the ratio of the total tangential force acting on the material to the total normal force exceeds the tangent of the wall friction angle, tan ϕ_w. The material will slide in the direction of the total tangential force (which will vary as the Cascade chamber rotates). Because force is proportional to acceleration, sliding will occur when

$$\tan \phi_w < \tan \alpha_{eff} = |a_t|/|a_n| \tag{2}$$

where $|a_t|$ and $|a_n|$ are the magnitudes of the tangential and normal acceleration.

Consider a frustum of a cone rotating on its horizontal axis with an angular velocity, ω, as shown in Figure 2. If we consider a relative frame of reference, from the point of view of a granule of material on the rotating surface, the centrifugal acceleration, $a_c = \omega^2 r$, always points radially outward, and the gravitational acceleration, g, appears to have its direction rotate about the axis. The radial acceleration, a_r, is the sum of the centrifugal acceleration and the sinusoidally varying projection of gravity in the radial direction. The normal acceleration is the projection of the radial acceleration perpendicular to the surface of the cone so that:

$$a_r = a_c + g \cos (\omega t) \tag{3}$$

$$|a_n| = |a_r| \cos \alpha = [\omega^2 r + g \cos (\omega t)] \cos \alpha \tag{4}$$

where r is the radius of the cone surface; t is time; ω is the angular velocity so that the angle θ, at the location of a granule on the surface, is equal to ωt; and α is the half-angle of the cone (see Fig. 2). The normal component of g varies with time, having a value of zero at the sides.

The total tangential acceleration, a_t, is composed of an axial component, a_a, acting axially along the cone surface, and a circumferential component, a_θ. The axial component is just the projection of the radial term, a_r, in the axial surface direction ($a_a = a_r \sin \alpha$). The circumferential component is composed of a gravity term and the Coriolis acceleration

$$a_\theta = - g \sin \theta - 2\omega v_r = - g \sin (\omega t) - 2\omega v_a \sin \alpha \tag{5}$$

where v_r and v_a are the radial and axial components of the granule velocity. The magnitude of tangential acceleration, $|a_t|$, and the angle, β, between a_t and the projection of the axis on the cone surface are

$$|a_t| = \sqrt{a_a^2 + a_\theta^2} =$$

$$\sqrt{[\omega^2 r + g\cos(\omega t)]^2 \sin^2\alpha + [-g\sin(\omega t) - 2\omega v_a \sin\alpha]^2}. \qquad (6)$$

$$\beta = \tan^{-1} a_\theta/a_a \qquad (7)$$

Conditions for sliding are determined from Equations (2), (4), and (6). If sliding does occur, then for any finite inclination angle, α, we can expect to see at least some axial motion because there will be a component of the tangential acceleration acting in the axial direction. Further, we expect to see an oscillating motion in the circumferential direction because the circumferential acceleration has a sinusoidal term.

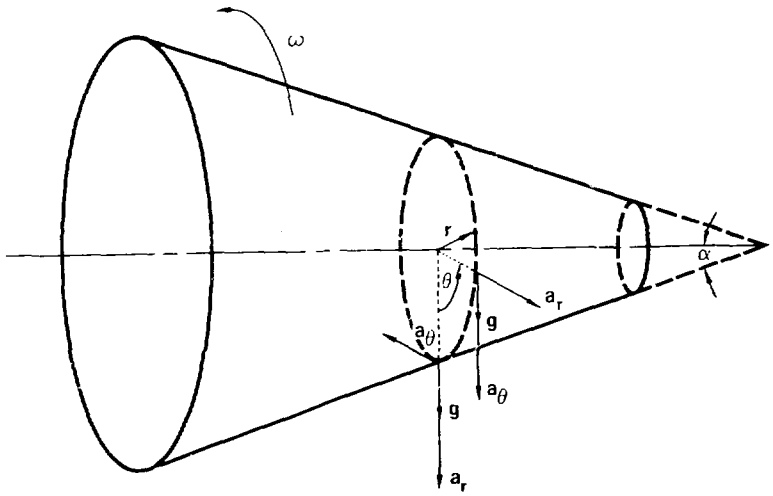

Fig. 2 Accelerations acting on granular material on the inside surface of a cone rotating on a horizontal axis is shown at two positions corresponding to $\theta = 0$ and $\theta = \pi/2$.

The value of $\omega^2 r$ will increase as a granule moves down the incline to a larger radius so that the constant amplitude, sinusoidally varying circumferential acceleration due to gravity will be a smaller fraction of $\omega^2 r$ at the large radii than it is at the small radii. Coriolis acceleration has a significant effect on both the Cascade chamber and on the laboratory-scale experiments described later, with the maximum effect existing when the granule is at the top ($\theta = \pi$), where the normal acceleration is a minimum.

We were also interested in mixing and granule size segregation in the flowing Cascade blanket because the energy deposition is an order of magnitude higher at the inside surface of the blanket than at the outside surface. Optimum operation calls for equal heating of all granules. One way of approaching that optimum is to ensure continuous mixing of the flowing granular bed as it moves, thereby constantly replacing the top surface layer that absorbs the bulk of the energy. Cascade's divergent flow geometry will force some shearing in the blanket and will cause mixing. It remains to be determined if the changing diameter of the chamber will produce enough mixing. One alternative is to incorporate partitions in the blanket or steps on the cone surface to increase shearing.

Results of our analysis as applied to the Cascade chamber, and one of our laboratory-scale experiments (the 40° - 20° double-angle cone) are summarized in Table 1. Note that the slide angle relative to the projection of the axis on the cone surface (the angle β) changes sign, being negative at the top, the bottom, and the right side, but positive at the left side. In both the Cascade chamber and the laboratory scale experiments, granules would oscillate circumferentially as they rotate around the cone and simultaneously move axially along the cone surface, increasing the desired mixing within the blanket. The effective cone angle, α_{eff}, is slightly more than the actual cone angle, α, with the largest difference existing in the entrance region of the full-scale Cascade chamber when $\theta = \pi/2$.

Table 1

Effective cone half-angle, α_{eff}, and slide angle relative to projection of the axis on the cone surface, β, for the full-scale Cascade chamber and one laboratory-scale cone experiment.

	Cascade chamber (5 m maximum radius, rotational speed of 30 rpm)		40° - 20° double-angle cone (43mm maximum radius, rotational of 500 rpm)	
Entrance region (α=40°)	α_{eff} (deg)	β (deg)	α_{eff} (deg)	β (deg)
θ = 0	40.1	-3.9	40.0	-1.0
$\pi/2$	48.1	-41.1	40.5	-10.4
π	40.6	-11.4	40.0	-1.3
$3\pi/2$	45.3	33.9	40.3	8.2
Exit region (α = 20°)				
θ = 0	20.0	-0.6	20.0	-0.6
$\pi/2$	23.0	-30.7	20.6	-14.3
π	20.0	-1.0	20.0	-0.8
$3\pi/2$	22.7	29.6	20.5	13.0

Laboratory-Scale Experiments

Our laboratory experiments consisted of clear lucite test cones rotating on their horizontal axes; the apparatus is shown in Fig. 3. Sand flowed through a metal tube into an inlet hopper, and flowed out the bottom of the hopper onto an auger driven by a drill motor. We could independently vary the rotational speed of both of the cone-shaped test section and the auger, and also vary the size of the opening in the bottom of the inlet hopper. All cones tested had a minimum inside radius of 25 mm and a maximum inside radius of 43 mm. Nominal rotational speed was 500 rpm. Cone half-angles ranged between 10° and 40°. The measured wall friction angle and angle of repose of sand were 24° and 37°, respectively.

Initial experiments were conducted with an unrestricted exit. When the 10° cone was rotated, we found that sand built up on the cone. The inner surface of the sand was also conical but the half angle was 35° (approximately equal to the angle of repose). Sand cascaded along the 35°

half-angle conical sand surface but appeared stationary below. Changes in rotational speed, which changed the centrifugal acceleration, had no effect as long as the speed was large enough to hold the sand against the cone. When the 20°, 30° or 40° cones were rotated, there was no sand buildup at all. Sand grains entering the small end of each cone immediately cascaded down the cone surface and out the large end.

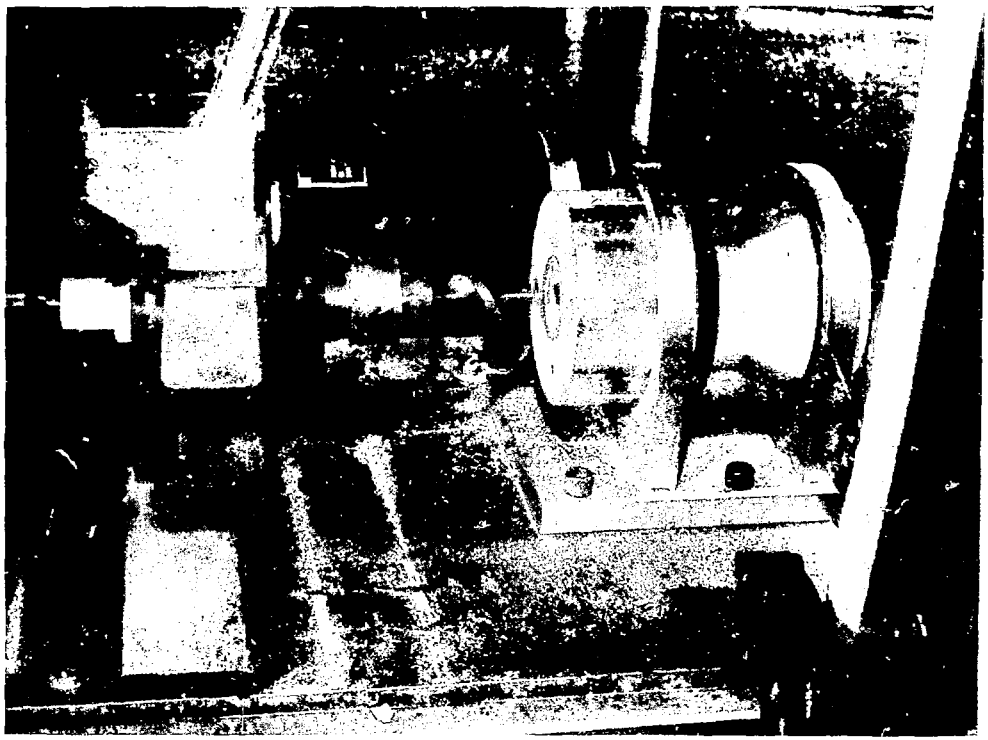

Fig. 3 Photograph of the experimental apparatus with the feed auger being installed into the cone shaped test section.

We had anticipated that sand would build up on the 20° cone in the same fashion as on the 10° cone because both angles are below ϕ_w. One possible explanation is that the feed auger interfered with the cone inlet region, so that the sand grains may never have accelerated to the wall

velocity before reaching the exit. Had our conical surface been longer, the sand might have built up on the 20° cone.

In our second series of tests, we added two-sided masking tape to the cones so that the inner surface of each cone was covered with a single layer of sand. When we rotated the cones, a stationary sand region built up not only on the 10° cone, but also on the 20° and 30° cones. In each of these cases the inside surface of the stationary sand region was also conical but with a half angle of 35°--just as it had been with the 10° cone without masking tape. With the 40° cone, no sand would build up regardless of whether or not there was two-sided masking tape attached to the cone surface.

We concluded that with a rough sand surface rigidly attached to the cone, sand grains cascading down the cone adhere to the sand below it until the angle of repose is reached. No sand layer built up on the 40° cone because this angle is above the 37° angle of repose. Again, results were independent of rotational speed.

In a final series of tests, we added an exit closure plate and fifteen equally spaced 2-mm x 3-mm exit apertures on the periphery. We tested both single- and double-angle cones, and obtained the results shown in Fig. 4. Sand built up to the angles shown. Although no measurements were taken, it appeared that the sand moved down the cone surface in slug flow and that the center portion of the cone was free of sand except for occasional grains kicked out into the center by the auger. An exception may have occurred in the 10° cone where the sand surface angle was the same as the 20° cone. In the 10° cone experiments, there may have been a layer of stationary sand next to the cone surface; we were unable to verify the existence of such a layer with the test equipment we used.

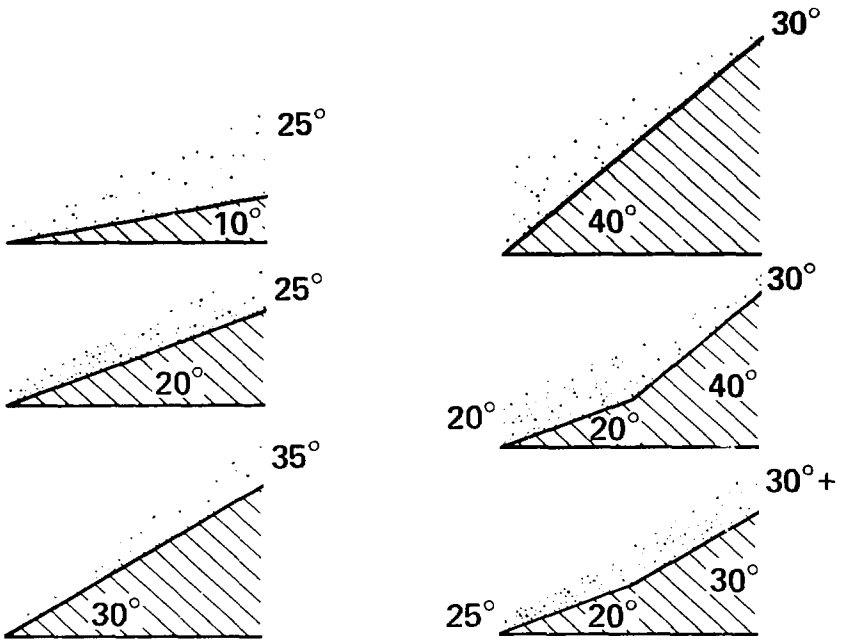

Fig. 4 Experimental sand profiles are shown for various rotating cone test sections. All cones tested had a minimum inside radius of 25 mm and a maximum inside radius of 43 mm. Nominal rotational speed was 500 rpm.

We found that for the closure-plate tests, the depth of sand on the cone surface was dependent on rotational speed. As rotational speed (and hence centrifugal acceleration) increased, the sand thickness decreased. We expected this phenomenon because granular flowrate through an orifice is proportional to the square root of the acceleration driving the flow.[5] Our inlet feed was held constant but the exit flowrate through the apertures depended on the centrifugal force, and hence thickness would change when rotational speed changed. We did find that the 40° single-angle cone and the 40° to 20° double-angle cone were particularly sensitive to rotational speed, perhaps because the 40° half-angle is above the angle of repose. We repeated this final series of tests with two-sided masking tape applied to the surfaces of the cones. Results were identical to those tests without tape.

From these tests we see that the thickness of the flowing layer decreases with distance down the cone when the cone-half-angle is less than the angle of repose and increases with distance when the cone-half-angle is greater than the angle of repose. A uniform thickness is desired for application to the Cascade chamber and although we did not test a cone with a half-angle exactly equal to the angle of repose for the material, we expect that at some cone-angle near the angle of repose it would be possible to obtain flows with constant thickness. With the 10° and 20° cones, we were able to control the sand depth ever though the cone half-angles were below the wall friction angle.

Conclusions:

We relate an effective cone half-angle, α_{eff}, to the actual cone half-angle, α, using centrifugal, gravitational, and Coriolis accelerations. The theory suggests that subcritical flow of cohesionless granular material can be controlled at the exit of a rotating cone if α_{eff} is between the wall friction angle, ϕ_w, and the angle of repose, φ_r. The granules oscillate circumferentially back and forth as they rotate around the cone and simultaneously move axially along the cone surface. This action increases mixing of the granules.

Laboratory-scale experiments with cones having half angles ranging from 10° to 40° show that exit control is possible over the entire range from $\phi_w < \alpha_{eff} < \phi_r$ and even beyond these limits. The most uniform granule layer is obtained when the half-angle of the cone is close to ϕ_r. Flowrate is dependent on the exit aperture area and the rotational speed.

Application of these results show the feasibility of a solid-granule blanket for the Cascade inertial-confinement fusion reaction chamber concept to convert fusion energy into electricity.

References:

1. J. H. Pitts, "Cascade: A Centrifugal-Action Solid-Breeder Reaction Chamber," Nucl. Technol./Fusion, vol. 4, No. 2, Part 2, Sept. 1983, pp. 967-972.

2. J. H. Pitts, "Shock Propagation Through the Cascade ICF Reactor Li_2O-Pebble Blanket," Trans. Am. Nucl. Soc., Vol. 45, 1983 Winter Meeting, San Francisco, CA, pp. 184-185.

3. J. H. Pitts, "Mechanical and Thermal Design of the Cascade Reactor," Proceedings, 10th Symposium on Fusion Engineering, Philadelphia, Penn., Dec. 1983, IEEE Cat. No. 83CH 1916-6, pp. 428-432.

4. O. R. Walton, "Granular Flow Considerations in the Design of a Cascade Solid-Breeder Reaction Chamber," Lawrence Livermore National Laboratory, Livermore, Calif. UCID-19903, Oct. 1983.

5. S. B. Savage and M. Sayed, "Gravity Flow of Cohesionless Granular Materials in Wedge-Shaped Hoppers," in Mechanics Applied to the Transport of Bulk Materials edited by S. C. Cowin, AMD-Vol. 31, pp. 1-24.